

Accounts

Structures and Magnetism of Cyanide-Bridged Bimetallic Compounds: Design of Complex-Based Magnetic Materials

Hisashi Ōkawa* **and Masaaki Ohba#**

Department of Chemistry, Faculty of Science, Kyushu University, Hakozaki, Higashiku 6-10-1, Fukuoka 812-8581

(Received August 21, 2001)

This account concerns the synthesis, structures and magnetism of cyanide-bridged bimetallic network compounds. The study aims at the development of molecular-based magnetic materials. Different network structures, from one-dimensional to three-dimensional, are synthesized by the reaction of $[M(CN)_6]^{n-}$ with a cationic constituent such as $[Ni(diamine)_2]^{2+}$, $[Ni(triamine)]^{2+}$, $[Mn(salen)]^{+}$, $[Mn(en)]^{2+}$, etc., in the absence or presence of an appropriate counter ion. Magnetostructural studies for those bimetallic compounds have clarified fundamental factors contributing to magnetic ordering in bulk, magnetic nature (ferromagnetism or metamagnetism) and magnetic phase-transition temperature (T_c). The strategies for gaining high T_c magnetic material and modulating magnetic nature by a change in network structure are described.

Systematic studies on molecular-based magnetic materials occurred at the end of the 1980's and three important magnetic systems were reported: one-dimensional charge-transfer complex $[Fe(Me_5cp)_2][TCNE]$ (Me_5cp^- = pentamethylcyclopentadienyl and TCNE = tetracyanoethylene) by Miller et al.,[1] one-dimensional oxamato-bridged bimetallic complex $\{MnCu(pbaOH)(H_2O)_3\}_x$ ($bpaOH^{4-}$ = 2-hydroxy-1,3-propylenedi(oxamate) anion) by Kahn et al.[2] and one-dimensional Mn^{II}-radical complex $\{M(hfa)_2(NITR)\}_x$ (hfa^- = hexafluoroacetylacetonate and NITR = 2-*R*-4,4,5,5-tetramethyl-4,5-dihydro-1-imidazolyl-1-oxy-3-oxide) by Gatteschi et al.[3] Stimulated by these pioneering works, the design of molecular magnetic materials using paramagnetic constituents is becoming a current research subject.[4–8] Metal complex constituents have great advantages over organic radical constituents, because electron spin(s) can be reserved to each metal center and different network structures of paramagnetic metal centers can be constructed by considering diverse stereochemistry of metal complexes. Furthermore, the magnetic nature of complex-based magnets can be chemically tuned by the choice of metal ion. A promising synthetic strategy for complex-based magnets is bimetallic networks that can be constructed by the reaction between a "complex bridge" having two or more groups capable of acting as bridges and a "coordinatively unsaturated complex" or simple metal ion. So far complex bridges of various types have been used for providing bimetallic network compounds exhibiting spontaneous magnetization.[7,8]

Among these complex bridges, hexacyanometallate(III), $[M(CN)_6]^{3-}$, is of particular interest since Prussian blue and analogs are known to form a family of magnetic materials.[9] Prussian blue itself shows a long-range ferromagnetic ordering (T_c = 5.6 K) in spite of involvement of diamagnetic Fe^{II},[10] and a high magnetic phase transition temperature was recognized for some Prussian blue analogs.[11–20] It is generally considered that Prussian blue and its analogs have a face-centered cubic structure, but this is based on statistical distribution of metal ions on the cubic lattice. In fact, detailed structural studies for Prussian blue family are very limited and the origin for the high T_c of some Prussian blue analogs remains unclear.

It is now known that $[M(CN)_6]^{n-}$ can take different bridging modes from μ^2 to μ^6 to provide bimetallic compounds of various network structures. Magnetostructural studies for those bimetallic compounds will serve to understand important factors contributing to magnetic ordering, magnetic nature (ferromagnetism or metamagnetism) and magnetic phase-transition temperature (T_c) and to provide a basis for developing new molecular magnetic materials.

1. One-Dimensional Network Compounds

(1) $[Ni(en)_2]_3[M(CN)_6]_2\cdot 2H_2O$ (M^{III} = Fe, Cr, Mn, Co). In our first study[21] *trans*-$[NiCl_2(en)_2]$ was reacted with $K_3[Fe(CN)_6]$ in the 3:2 stoichiometry in an aqueous solution to result in the immediate precipitation of polycrystalline samples of $[Ni(en)_2]_3[Fe(CN)_6]_2\cdot 2H_2O$. Good crystalline samples of $[Ni(en)_2]_3[M(CN)_6]_2\cdot 2H_2O$ (M^{III} = Cr, Mn, Fe, Co) were obtained by the reaction of $[Ni(en)_3]Cl_2$ and $K_3[M(CN)_6]$ in an aqueous solution.[22] In this reaction, the low dissociation of $[Ni(en)_3]^{2+}$ into $[Ni(en)_2]^{2+}$ in water leads to slow growth of

PRESTO (JST)

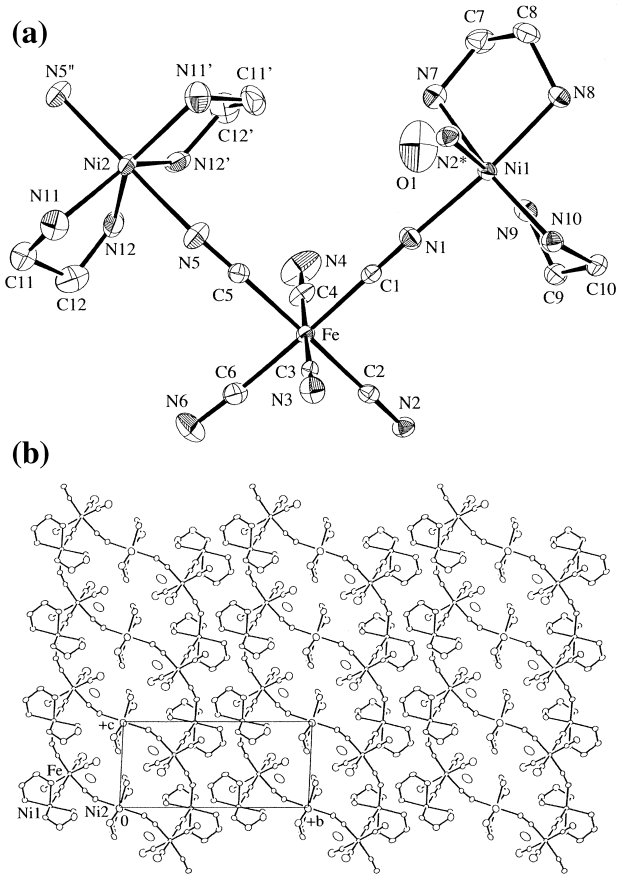

Fig. 1. (a) Asymmetric unit structure and (b) a projection of ladder structure of $[Ni(en)_2]_3[Fe(CN)_6]_2{\cdot}2H_2O$.

single crystals suitable for X-ray crystallographic studies. This synthetic method using tris(diamine)nickel(II), $[Ni(diamine)_3]^{2+}$, has proved to be applicable to various cyanide-bridged bimetallic compounds with bis(diamine)nickel(II), $[Ni(diamine)_2]^{2+}$, as the cationic constituent described below.

The asymmetric unit of $[Ni(en)_2]_3[Fe(CN)_6]_2{\cdot}2H_2O$ consists of one $[Fe(CN)_6]^{3-}$ anion, one *cis*-$[Ni(en)_2]^{2+}$ cation, one half of *trans*-$[Ni(en)_2]^{2+}$ cation, and one water molecule (Fig. 1 (a)).[22] $[Fe(CN)_6]^{3-}$ coordinates to two *cis*-$[Ni(en)_2]^{2+}$ and one *trans*-$[Ni(en)_2]^{2+}$ cations with its three cyanide groups in the *mer* mode. A 1-D zigzag chain is formed by the alternate array of *cis*-$[Ni(en)_2]^{2+}$ and $[Fe(CN)_6]^{3-}$, and two zigzag chains are combined by *trans*-$[Ni(en)_2]^{2+}$ providing a ladder structure (Fig. 1 (b)). The adjacent Fe···Ni1 and Fe···Ni2 separations in the ladder are 5.145 and 4.993 Å, respectively.

The $\chi_M T$ value of a crystalline sample of $[Ni(en)_2]_3[Fe(CN)_6]_2{\cdot}2H_2O$ is 4.95 cm^3 K mol^{-1} (6.29 μ_B) per Ni_3Fe_2 at room temperature and the $\chi_M T$ value increased with decreasing temperature to a maximum value of 10.22 cm^3 K mol^{-1} (9.04 μ_B) at 14 K and then decreased below this temperature (Fig. 2, a).[22] The maximum value is close to the spin-only value (10.0 cm^3 K mol^{-1}, 8.94 μ_B) for $S_T = 4$ indicating a ferromagnetic interaction between the adjacent low-spin Fe^{III} and high-spin Ni^{II} ions. The significance of the $d_\pi(M)$-$p_\pi(CN)$ interaction in $[M(CN)_6]^{3-}$ (M^{III} = Fe, Cr) which affords a large spin density on the p_π orbital of cyanide nitrogen is well known,[23,24] and the ferromagnetic interaction observed for $[Ni(en)_2]_3[Fe(CN)_6]_2{\cdot}2H_2O$ can be rationalized by the strict orthogonality of the magnetic orbitals of low-spin Fe^{III} (t_{2g}^1) and Ni^{II} (e_g^2), i.e., $d_\pi(Fe) \parallel p_\pi(CN) \perp d_\sigma(Ni)$. The drop in $\chi_M T$ value below 14 K suggests an antiferromagnetic interaction between the ladder chains. No magnetic ordering occurs over the lattice in the crystalline sample.

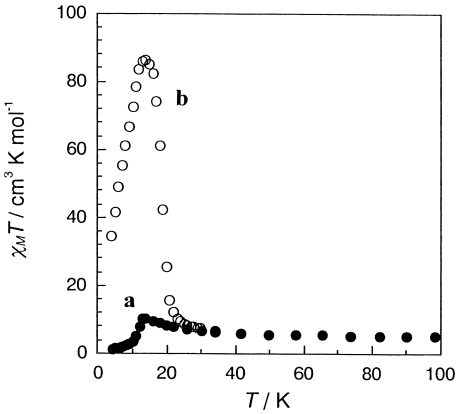

Fig. 2. $\chi_M T$ vs T plots of (a) crystalline and (b) polycrystalline samples of $[Ni(en)_2]_3[Fe(CN)_6]_2{\cdot}2H_2O$.

A polycrystalline sample of $[Ni(en)_2]_3[Fe(CN)_6]_2{\cdot}2H_2O$ markedly differs from the crystalline sample in magnetic nature.[21] Its $\chi_M T$ value increased sharply below 20 K up to a large maximum value of 86.1 cm^3 K mol^{-1} (26.2 μ_B) at 14 K (Fig. 2, b). Magnetization studies (field-cooled magnetization (FCM), zero-field-cooled magnetization (ZFCM), remnant magnetization (RM)) demonstrated a ferromagnetic ordering over the lattice below 18.6 K. It must be mentioned that the crystalline and polycrystalline samples give the same IR and powder X-ray diffraction spectra. Three ν(CN) vibrations are observed at 2150, 2130 and 2110 cm^{-1}. The last band is well compared to the ν(CN) band of $K_3[Fe(CN)_6]$ (2110 cm^{-1}). It is generally known that ν(CN) band shifts to higher frequency on bridge formation.[9] Thus, the former two bands at 2150 and 2130 cm^{-1} are ascribed to bridging cyanide groups.

The above result warns us that a polycrystalline sample can have a disorder in network structure and magnetic property often reflects the disordered local domains. In the present case, the polycrystalline sample of $[Ni(en)_2]_3[Fe(CN)_6]_2{\cdot}2H_2O$, prepared by rapid precipitation in the reaction between $[Fe(CN)_6]^{3-}$ and $[Ni(en)_2]^{2+}$, has a disorder in the ladder network and the magnetic ordering arises from the resulting pseudo 2-D or 3-D domain. Difference in magnetic property between crystalline and polycrystalline samples was also recognized for $[Ni(bpm)_2]_3[Fe(CN)_6]{\cdot}7H_2O$ (bpm = bis(1-pyrazolyl)methane) by Murray et al.[25]

Similarly, crystalline samples of $[Ni(en)_2]_3[Cr(CN)_6]_2{\cdot}2H_2O$ and $[Ni(en)_2]_3[Mn(CN)_6]_2{\cdot}2H_2O$ show a ferromagnetic interaction in the 1-D ladder but no magnetic ordering in the bulk.[21] $[Ni(en)_2]_3[Co(CN)_6]_2{\cdot}2H_2O$ is paramagnetic because Co^{III} has no unpaired electron.

The Weiss constants (θ) of the Ni_3Fe_2, Ni_3Mn_2 and Ni_3Cr_2 compounds were evaluated to be +6.3, +13.8 and +18.4 K, respectively, by Curie–Weiss plots ($1/\chi_M = (T-\theta)/C$) in the higher temperature region. Evidently the ferromagnetic interaction between the adjacent Ni^{II} and M^{III} ions through the cya-

nide bridge becomes stronger with the increase of unpaired electrons on the M^{III} ion.

(2) $PPh_4[Ni(pn)_2][M(CN)_6]\cdot H_2O$ (M^{III} = Fe, Cr, Co). These complexes were obtained as prismatic crystals by the reaction of $[Ni(pn)_3]Cl_2$ and $K_3[M(CN)_6]$ in an aqueous solution in the presence of tetraphenylphosphonium chloride PPh_4Cl.[26,27] They are isomorphous and show two ν(CN) bands at ~2130 and ~2110 cm^{-1}. The former band is attributed to bridging cyanide group and the latter band to non-bridging cyanide group in comparison with IR spectra of $K_3[M(CN)_6]$. The asymmetric unit structure of $PPh_4[Ni(pn)_2][Cr(CN)_6]\cdot H_2O$ is given in Fig. 3, (a). Each $[Cr(CN)_6]^{3-}$ makes bonds to two $[Ni(pn)_2]^{2+}$ cations through two cyanide groups in *cis*, affording a 1-D zigzag chain structure with the alternate array of $[Ni(pn)_2]^{2+}$ and $[M(CN)_6]^{3-}$ ions (Fig. 3 (b)). The adjacent Cr···Ni separation is 5.215(1) Å. In the three isomorphous complexes, the average M–C bond distance increases in the order: M = Co (1.927 Å) < Fe (1.964 Å) < Cr (2.077 Å). This is in the order of decreasing number of d_π electrons at the metal center, indicating the significance of π-back donation from the d_π orbital of M^{III} to the vacant orbital of cyanide ion.

The $\chi_M T$ value of the NiFe compound slightly decreased on lowering temperature to a minimum value near 50 K and then increased to a maximum value of 2.38 cm^3 K mol^{-1} (4.36 μ_B) at 5.0 K. The first decrease in $\chi_M T$ from 300 K to 50 K is typical of the $^2T_2$ term of low-spin Fe^{III} under Oh symmetry. The maximum $\chi_M T$ value at 5.0 K is common for ferromagnetically coupled Fe^{III}(S = 1/2)–Ni^{II}(S = 1); the value of 2.06 – 2.47 cm^3 K mol^{-1} (4.06 – 4.44 μ_B) is expected for S_T = 3/2 using g = 2.1 – 2.3. Thus no long-range magnetic ordering occurs over the lattice in this compound.

In the case of the NiCr compound, the $\chi_M T$ value sharply increased with decreasing temperature to a maximum value of 12.35 cm^3 K mol^{-1} (9.94 μ_B) at 7.0 K and then decreased. The maximum $\chi_M T$ value is larger than the spin-only value for S_T = 5/2 arising from ferromagnetic coupling between Cr^{III}(S = 3/2) and Ni^{II}(S = 1) (4.38 cm^3 K mol^{-1}; 5.92 μ_B). This suggests a long-range magnetic ordering in the bulk, but no remnant magnetization was observed at 4.2 K. The NiCo compound showed paramagnetic nature over the temperature range of 4.2 – 300 K.

(3) Other Complexes. The reaction of $[Mn(acacen)]^+$ with $[Fe(CN)_6]^{3-}$ formed $(NEt_4)_2[Mn(acacen)][Fe(CN)_6]$, which has a 1-D chain structure with an alternating array of $[Mn(acacen)]^+$ and $[Fe(CN)_6]^{3-}$.[28] A ferromagnetic interaction occurs between the adjacent high-spin Mn^{III} and low-spin Fe^{III} through cyanide bridge. Both antiferromagnetic and ferromagnetic interactions are expected for cyanide-bridged Fe^{III}–Mn^{III} compounds depending upon the geometry of the dinuclear $Mn^{III}(t_{2g}^3e_g^1)$–NC–$Fe^{III}(t_{2g}^1)$ unit. Antiferromagnetic interaction can occur by the superexchange mechanism of d_{xz}(Fe) ‖ p_x(CN) ‖ d_{xz}(Mn) (or d_{yz}(Fe) ‖ p_y(CN) ‖ d_{yz}(Mn)) when the local x and y axes about Fe^{III} and the local x′ and y′ axes about Mn^{III} are coincident with respect to the Fe–CN–Mn linkage (common z axis) (Fig. 4(a)).[29] If the local axes x′ and y′ are rotated by 45° about the Fe–CN–Mn linkage, the strict orthogonality holds between the magnetic orbitals of the two metal ions because of d_{xz}(Fe) ‖ p_x(CN) ⊥ $d_{x'z}$(Mn) (Fig. 4(b)). This is the case of $(NEt_4)_2[Mn(acacen)][Fe(CN)_6]$ which exhibits a ferromagnetic interaction between the adjacent Mn^{III} and Fe^{III} ions. In this compound a weak ferromagnetic interaction oper-

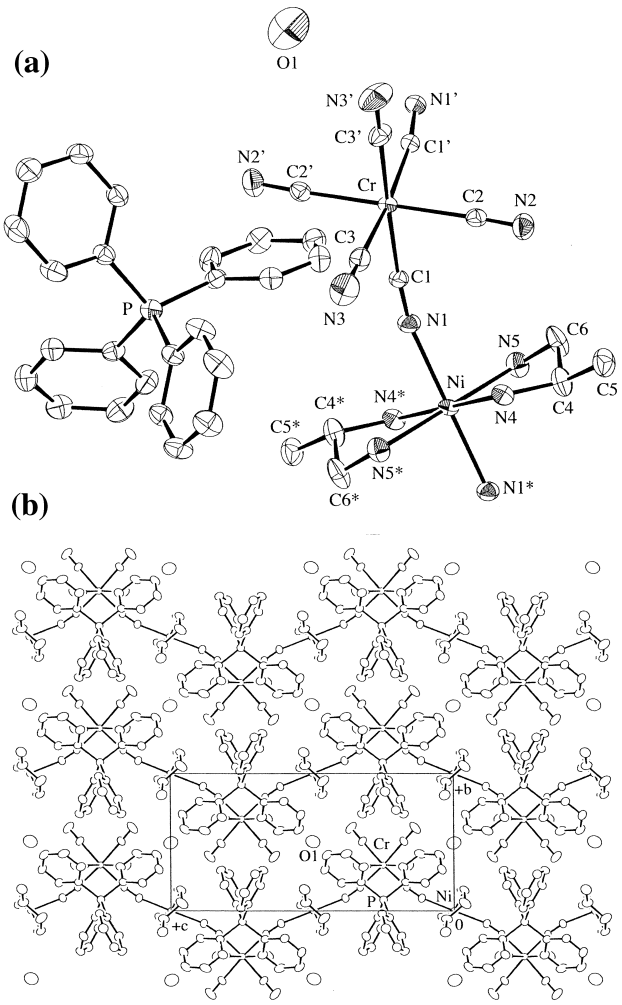

Fig. 3. (a) Asymmetric unit structure and (b) a projection of chain structure of $PPh_4[Ni(pn)_2]_3[Fe(CN)_6]\cdot H_2O$.

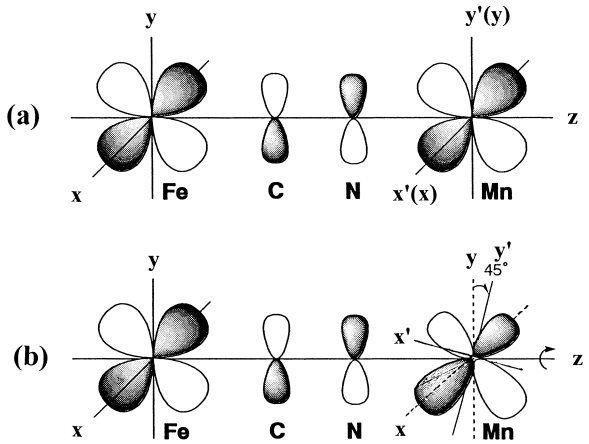

Fig. 4. Two spin-exchange mechanisms affording (a) antiferromagnetic and (b) ferromagnetic interaction in $(CN)_5Fe^{III}$–CN–Mn^{III}(SB).

ates among the 1-D chains to show a tendency of magnetic ordering below 2.5 K.

$[Fe^{III}(cyclam)][Fe^{III}(CN)_6]\cdot 6H_2O$ was obtained by the reaction of $[Ni(cyclam)][Fe(CN)_6]\cdot 6H_2O$ with a large excess of $[Fe(CN)_6]^{3-}$ in an aqueous solution.[30] It was also prepared by the reaction of cyclam and $K_3[Fe(CN)_6]$ in aqueous solution. It consists of 1-D linear chains with alternating array of $[Fe(CN)_6]^{3-}$ and $[Fe(cyclam)]^{3+}$ ions and shows a ferromagnetic interaction within the 1-D chain. A careful examination of the structure reveals that the coordination polyhedron of the $\{Fe(cyclam)(N)_2\}$ part (*N*: cyanide nitrogen from adjacent $[Fe(CN)_6]^{3-}$) is elongated along the CN–Fe–NC direction (D_{4h}). Under D_{4h} symmetry, the ground state configuration of the low-spin Fe^{III} is depicted as $(d_{xy})^1$ (the z axis is taken along the CN–Fe–NC linkage). Thus, the ferromagnetic interaction might be the result of orthogonality between the d_{xz} and d_{yz} orbitals of $[Fe(CN)_6]^{3-}$ (Fe(1)) and d_{xy} orbital of $\{Fe(cyclam)(N)_2\}$ (Fe(2)), i. e., $d_{xz}(Fe(1)) \parallel p_x(CN) \perp d_{xy}(Fe(2))$. No magnetic ordering occurs in this compound.

$[Cu(dien)]_3[Fe(CN)_6]_2\cdot 6H_2O$ (dien = diethylenetriamine) was obtained when $[Cu(dien)]^{2+}$ was used as the cationic constituent.[31] The $\{Cu(dien)\}^{2+}$ unit in a five-coordinate geometry provides two vacant sites for accepting cyanide nitrogens from adjacent $[Fe(CN)_6]^{3-}$ anions. A 1-D chain consisting of $\{Cu(dien)\}_2\{Fe(CN)_6\}^+$ cations is formed, and dinuclear $[Cu(dien)(H_2O)Fe(CN)_6]^-$ anions exist among the 1-D chains. A weak ferromagnetic interaction operates between the adjacent metal ions due to $d_\pi(Fe) \parallel p_\pi(CN) \perp d_\sigma(Cu)$, but no magnetic ordering occurs in the lattice.

In summary, cyanide-bridged 1-D bimetallic compounds generally show no magnetic ordering in the bulk, though a tendency of magnetic ordering was recognized in limited cases. The crucial step to realize magnetic ordering based on 1-D ferromagnetic or ferrimagnetic chains is how to control the phase of 1-D chains so as to achieve a three-dimensional magnetic ordering of spins. No principle for controlling interchain interaction has been established so far.

2. Two-Dimensional Network Compounds

(1) $[Ni(N\text{-men})_2]_3[M(CN)_6]_2\cdot nH_2O$ (*N*-men = *N*-Methylethylenediamine; M^{III} = Fe, Co). The 1-D ladder structure of $[Ni(en)_2]_3[M(CN)_6]_2\cdot 2H_2O$ (M = Cr, Mn, Fe, Co) relates to $[Ni(en)_2]^{2+}$ that is capable of affording both *cis*-$\{Ni(en)_2(N)_2\}$ unit and *trans*-$\{Ni(en)_2(N)_2\}$ unit in the network (cf. Fig. 1). If $[Ni(diamine)_2]^{2+}$ affords only one geometrical form (*cis*- or *trans*-$\{Ni(diamine)_2(N)_2\}$) owing to a requirement of the diamine ligand, a different network structure must be derived.

$[Ni(N\text{-men})_2]_3[M(CN)_6]_2\cdot nH_2O$ (M = Fe, Co) were prepared by the reaction of $[Ni(N\text{-men})_3]Cl_2$ and $K_3[M(CN)_6]$ in aqueous solution.[32] The $[M(CN)_6]^{3-}$ anion bonds to three $[Ni(N\text{-men})_2]^{2+}$ cations through three cyanide groups in *mer* mode, providing a 2-D sheet structure based on cyclic Ni_6M_6 units (Fig. 5). The unit forms a honeycomb-like hexagon with the M^{III} at each corner and Ni^{II} at the middle of each edge. The nearest Fe···Fe, Ni···Ni and Ni···Fe separations in the sheet of the Ni_3Fe_2 compound are 8.916(3), 8.916(3) and 7.843(3) Å, respectively. The $\{Ni(N\text{-men})_2(N)_2\}$ moiety assumes trans configuration due to steric effect of the *N*-methyl group. The crystalline sample has at least fifteen water molecules within the hexagonal unit.

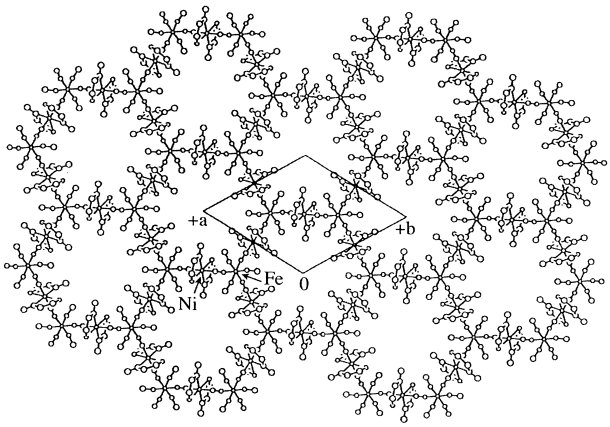

Fig. 5. A projection of 2-D honeycomb sheet structure of $[Ni(N\text{-men})_2]_3[Fe(CN)_6]_2\cdot 15H_2O$.

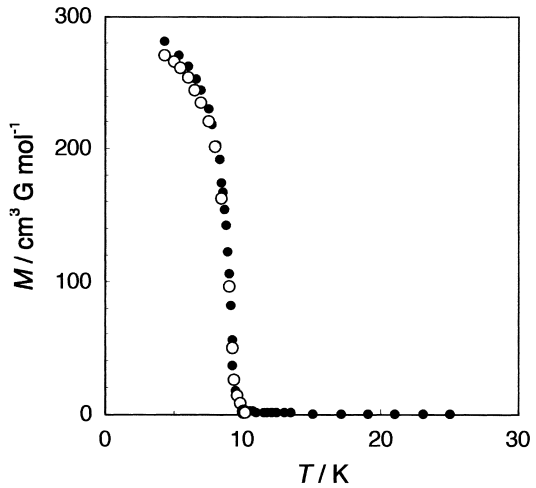

Fig. 6. FCM (●) and RM (○) of $[Ni(N\text{-men})_2]_3[Fe(CN)_6]_2\cdot 15H_2O$.

The Ni_3Fe_2 complex was partially dehydrated in open air to give $[Ni(N\text{-men})_2]_3[Fe(CN)_6]_2\cdot 12H_2O$ for which magnetic studies were made. The $\chi_M T$ value per Ni_3Fe_2 is 471 cm^3 K mol^{-1} (6.13 μ_B) at room temperature, and the $\chi_M T$ value increased with decreasing temperature to a large value of 79.7 cm^3 K mol^{-1} (25.4 μ_B) at 7.0 K and then decreased below this temperature. Magnetization studies (FCM, RM and ZFCM) have demonstrated a ferromagnetic ordering in the bulk (T_c = 10.8 K) (Fig. 6). On the other hand, anhydrous $[Ni(N\text{-men})_2]_3[Fe(CN)_6]_2$, prepared by heating the hydrated sample at 100 °C in vacuo, showed no magnetic ordering in the bulk. The result suggests that the 2-D honeycomb sheet structure is broken on dehydration. In this connection, very efflorescent $[Ni(cyclam)]_3[Cr(CN)_6]_2\cdot 20H_2O$ (cyclam = 1,4,8,11-tetraazacyclotetradecane) has a similar honeycomb sheet structure, but the amorphous pentahydrate, $[Ni(cyclam)]_3[Cr(CN)_6]_2\cdot 5H_2O$, obtained in open air showed no magnetic ordering.[33]

(2) $[Ni(chxn)_2]_3[M(CN)_6]_2\cdot 2H_2O$ (chxn = 1, 2-*trans*-Cyclohexanediamine; M^{III} = Fe, Co). These compounds were obtained by the reaction of $[Ni(chxn)_3]Cl_2$ and $K_3[M(CN)_6]$ in an aqueous solution.[34] $[Ni(chxn)_2]_3[Fe(CN)_6]_2\cdot 2H_2O$ shows

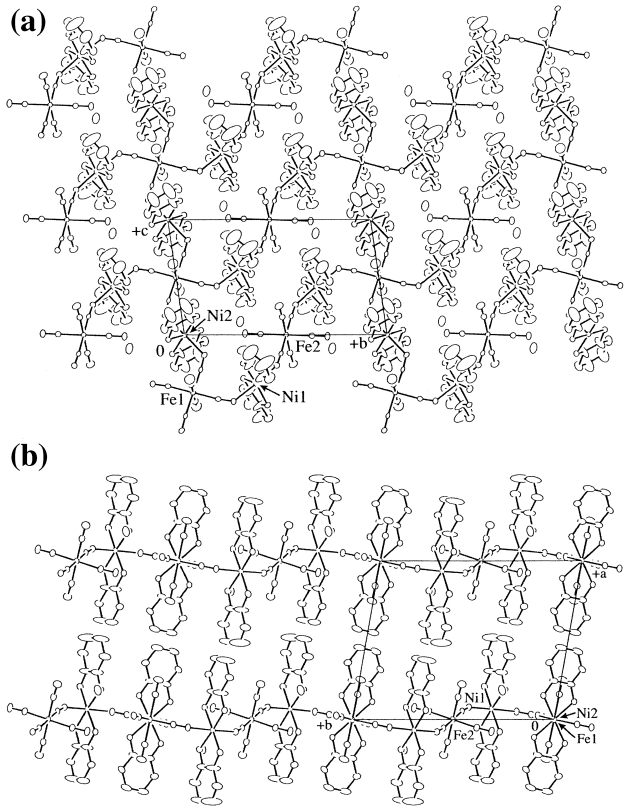

Fig. 7. 2-D network structure of $[Ni(chxn)_2]_3[Fe(CN)_6]_2 \cdot 2H_2O$; (a) a top view and (b) a side view.

three ν(CN) bands at 2122, 2115 and 2105 cm^{-1} and $[Ni(chxn)_2]_3[Co(CN)_6]_2 \cdot 2H_2O$ also shows three ν(CN) bands at 2139, 2131 and 2116 cm^{-1}. In the crystal of $[Ni(chxn)_2]_3[Fe(CN)_6]_2 \cdot 2H_2O$ there exist two types of $[Fe(CN)_6]^{3-}$ anions, μ^4-$[Fe1(CN)_6]^{3-}$ and μ^2-$[Fe2(CN)_6]^{3-}$. The alternate array of $[Ni1(chxn)_2]^{2+}$, μ^4-$[Fe1(CN)_6]^{3-}$, $[Ni1(chxn)_2]^{2+}$ and μ^2-$[Fe2(CN)_6]^{3-}$ forms a 1-D chain along b axis and, the chains are combined by $[Ni2(chxn)_2]^{2+}$ cations along c axis (Fig. 7). The resulting network is a 2-D sheet comprised of Ni_6Fe_6 dodecagon units in a distorted parallelogram. The nearest intersheet Fe···Fe (= Ni···Ni) separation is 12.717(3) Å.

The $\chi_M T$ value for the Ni_3Fe_2 compound is 4.24 cm^3 K mol^{-1} (5.83 μ_B) at room temperature and increased with decreasing temperature to a large maximum value of 652 cm^3 K mol^{-1} (72.2 μ_B) at 12 K. A ferromagnetic ordering in the bulk has been demonstrated based on magnetization studies (T_c = 13.1 K).

(3) $[Ni(tren)]_3[Fe(CN)_6]_2 \cdot 6H_2O$ (tren = Tris(2-aminoethyl)amine). The use of $[Ni(tren)]^{2+}$ as the cationic constituent is of interest because $[Ni(tren)]^{2+}$ provides two vacant sites in cis for accepting cyanide nitrogen from $[Fe(CN)_6]^{3-}$.[35] In the crystal there are two types of $[Fe(CN)_6]^{3-}$ groups, μ^4-$[Fe(CN)_6]^{3-}$ and μ^2-$[Fe(CN)_6]^{3-}$. The chains parallel to b and c axes are composed of Ni–(μ^4-Fe)–Ni–(μ^2-Fe)-Ni linkages, and each μ^4-Fe unit belongs to two different orthogonal chains. The chains parallel to a axis are build up from Ni–(μ^2-Fe)–Ni linkages. The resulting network is apparently three-dimensional, but the magnetic nature is essentially of 2-D type showing a magnetic ordering at T_c = 8 K. No magnetic interaction

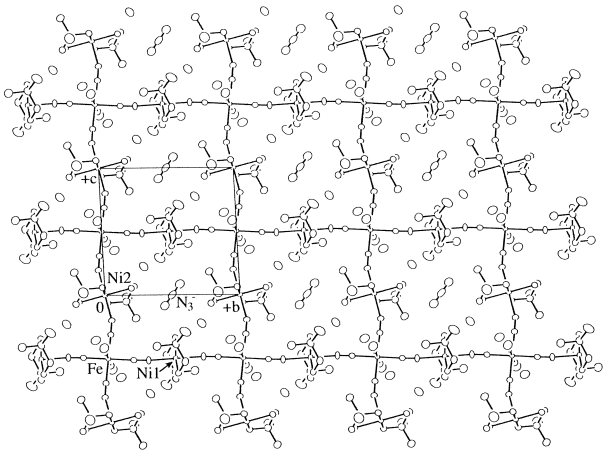

Fig. 8. A projection of 2-D square sheet structure of $[Ni(1,1\text{-dmen})_2]_2[Fe(CN)_6]N_3 \cdot 4H_2O$.

along the a axis is supposed because of an elongation of the Fe–CN–Ni linkage along this axis.

(4) $[Ni(L)_2]_2[Fe(CN)_6]X \cdot nH_2O$ (L = pn, 1, 1-dmen; X^- = Counter Anion). These compounds were prepared by the reaction of $[Ni(L)_3]X_2$ and $K_3[Fe(CN)_6]$ in aqueous solution.[36–38] The compounds with L = pn were obtained with limited counter anions (ClO_4^-, BF_4^-, PF_6^-), whereas those with L = 1, 1-dmen were obtained with various anions (ClO_4^-, BF_4^-, PF_6^-, $CF_3SO_3^-$, BzO^-, I^-, N_3^-, NCS^-, NO_3^-). They have two ν(CN) modes near 2140 and 2110 cm^{-1}, attributable to the bridging and non-bridging CN^- groups, respectively. X-ray crystallographic studies have revealed that each $[Fe(CN)_6]^{3-}$ makes bonds to four $[Ni(L)_2]^{2+}$ cations with its four cyanide groups on a plane to afford a 2-D grid structure (Fig. 8). The 2-D sheet is based on a Ni_4Fe_4 square unit with Fe^{III} ion at each corner and Ni^{II} ion at the middle of each edge of the square. The methyl substituent(s) on the ethylene backbone of the diamine ligand forms a fence around the square cavity so as to accommodate the counter anion within the cavity.

All the complexes show a ferromagnetic interaction within the 2-D sheet and a long-range magnetic ordering over the lattice. The magnetic nature in the bulk is ferromagnetism or metamagnetism depending upon the intersheet separation. Metamagnetism occurs when the intersheet separation is small so as to cause an antiferromagnetic interaction between the 2-D sheets. This is the case of $[Ni(pn)_2]_2[Fe(CN)_6]ClO_4 \cdot 2H_2O$ with an intersheet separation of 8.613 Å. Its $\chi_M T$ value at room temperature is 3.21 cm^3 K mol^{-1} per Ni_2Fe (5.07 μ_B), which increased upon cooling to a maximum value of 12.21 cm^3 K mol^{-1} (9.88 μ_B) at 10 K and then decreased below 10 K (Fig. 9, left a). The saturation magnetization curve at 4.2 K showed a break characteristic of metamagnet around 3800 G (Fig. 9, right a). The break means that the intersheet antiferromagnetic interaction is overcome by an external field of ~4000 G to cause the spin flip for ferromagnetic ordering.

Ferromagnetism occurs, for example, in $[Ni(1,1\text{-dmen})_2]_2[Fe(CN)_6]CF_3SO_3 \cdot 2H_2O$ that has an intersheet separation of 9.91 Å. Its $\chi_M T$ vs T curve has a large maximum of 312.9 cm^3 K mol^{-1} (50.0 μ_B) at 8.5 K and the χ_M vs T curve showed no decrease at low temperature (Fig. 9, left b). The on-set of a long-range magnetic ordering was demonstrated by magneti-

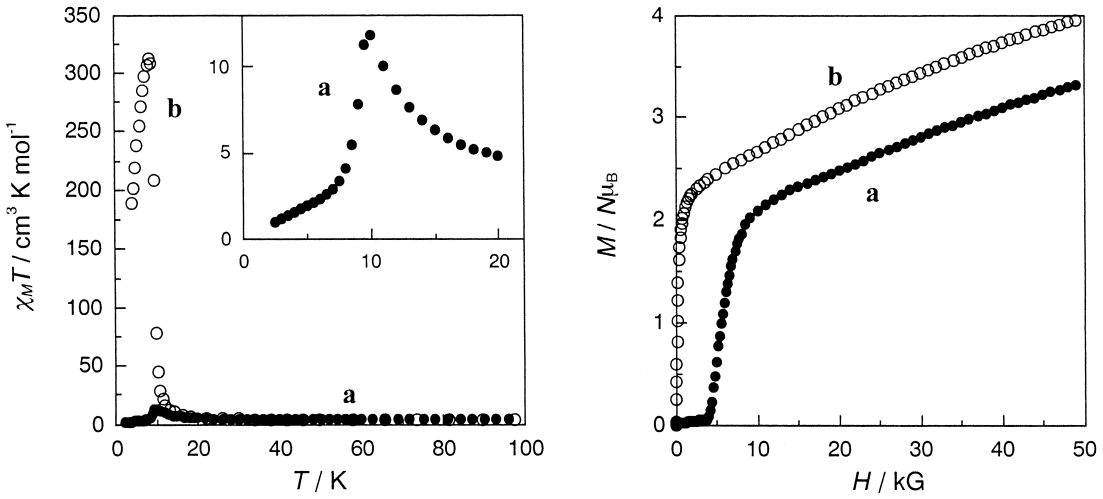

Fig. 9. Temperature-dependence of $\chi_M T$ (left) and field-dependence of magnetization at 2 K (right) for (a) $[Ni(pn)_2]_2[Fe(CN)_6]ClO_4 \cdot 2H_2O$ and (b) $[Ni(1,1\text{-dmen})_2]_2[Fe(CN)_6]CF_3SO_3 \cdot 2H_2O$.

Table 1. Magnetic Properties of $[Ni(L)_2]_2[Fe(CN)_6]X \cdot nH_2O$

Hydrated sample					Dehydrated sample	
L	X^-	n	Magnetism	δ/Å	n	Magnetism
pn	ClO_4^-	2	meta	8.613		
pn	BF_4^-	2	meta			
pn	PF_6^-	2	meta			
1,1-dmen	ClO_4^-	2	meta		0	meta
1,1-dmen	BF_4^-	3	ferro		0	meta
1,1-dmen	PF_6^-	2	meta		1	meta
1,1-dmen	$CF_3SO_3^-$	2	ferro	9.91	0	meta
1,1-dmen	BzO^-	6	ferro	11.1, 10.4	1	meta
1,1-dmen	I^-	4	ferro		0	meta
1,1-dmen	N_3^-	4	ferro	10.158	0	meta
1,1-dmen	NCS^-	1	meta		0	meta
1,1-dmen	NO_3^-	4	ferro		–	

δ = intersheet separation; meta = metamagnetism; ferro = ferromagnetism

zation studies (T_c = 9.5 K). The saturation magnetization curve showed a sharp increase with applied field (Fig. 9, right b).

The magnetic properties of the 2-D bimetallic complexes are summarized in Table 1. The intersheet separation depends upon the diamine ligand, the counter anion and the number of lattice water molecules. All the complexes with L = pn are metamagnets irrespective of counter anion, because of less bulkiness of the pn ligand and a small number of lattice water molecules (n = 2). In the compounds with the moderately bulky 1,1-dmen ligand, the counter ion and the number of hydrated water molecules are both important in determining the inter-sheet separation. In general, the existence of three or more molecules of hydrated water leads to a significant intersheet separation and thence a ferromagnetic ordering occurs. One exception is $[Ni(1,1\text{-dmen})_2]_2[Fe(CN)_6]CF_3SO_3 \cdot 2H_2O$, which shows ferromagnetic ordering in spite of two molecules of hydrated water. In this compound the $CF_3SO_3^-$ ion in the square cavity is situated perpendicularly to the 2-D sheet and contributes to a significant intersheet separation (9.91 Å).

The significance of hydrated water in determining the intersheet separation was supported by dehydration studies for the ferromagnetic compounds with the 1,1-dmen ligand. The dehydrated samples of the ferromagnetic compounds, anhydrate or monohydrate, were found to exhibit metamagnetic nature. Evidently, the dehydration results in shortening the intersheet separation and thence enhancing the intersheet antiferromagnetic interaction.

$[Ni(1,1\text{-dmen})_2]_2[Fe(CN)_6](p\text{-}TolSO_3) \cdot 2H_2O$ (p-$TolSO_3$ = p-methylbenzenesulfonate ion) and $[Ni(1,\ 1\text{-dmen})_2]_2[Fe(CN)_6](p\text{-}PhBSO_3) \cdot 4H_2O$ (p-$PhBSO_3$ = p-phenylbenzenesulfonate ion) are both ferromagnets (T_c = 10.7 and 9.5 K, respectively) in accord with a large intersheet separation (11.46 Å for the former and 12.80 Å for the latter).[39] These compounds are not converted into metamagnets on dehydration because the anions are bulky enough to retain a large intersheet separation (> ca. 10 Å) even in the dehydrated form.

Analogous compounds with L = en, $[Ni(en)_2]_2[Fe(CN)_6]X$ (X = ClO_4^-, BF_4^-, PF_6^-), show a short-range ferromagnetic interaction between the adjacent Ni^{II} and Fe^{III} ions but no magnetic ordering over the lattice.[38] A 1-D structure is supposed for these compounds based on the observation of three ν(CN) bands at 2140, 2130 and 2110 cm^{-1}.[21,22] It must be mentioned that the 2-D square sheet compounds mentioned above have

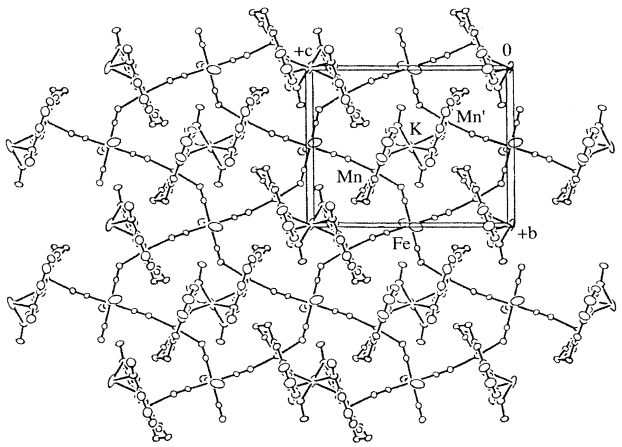

Fig. 10. 2-D network of K[{Mn(3-MeOsalen)}$_3${Fe(CN)$_6$}]·2DMF.

two ν(CN) modes near 2140 and 2110 cm^{-1}.[38] It is likely that the square cavity formed with $[Ni(en)_2]^{2+}$ is too shallow to accommodate a large counter ion (ClO_4^-, BF_4^- and PF_6^-). On the other hand, $[Ni(en)_2]_2[Fe(CN)_6]NO_3\cdot 3H_2O$ and $[Ni(tn)_2]_2[Fe(CN)_6]NO_3\cdot 2H_2O$ show a metamagnetic ordering.[40] A 2-D sheet structure like that of Fig. 8 has been confirmed for the latter compound in which planar NO_3^- ion is accommodated within the shallow square cavity.

(5) A[Mn(SB)]$_2$[M(CN)$_6$]·*n*H$_2$O (SB = Tetradentate Schiff Bases). The reaction of $[Mn(SB)(H_2O)]ClO_4$ with $K_3[Fe(CN)_6]$ gave two types of compounds: $K[Mn(SB)]_2[Fe(CN)_6]$ and $[\{Mn(SB)\}_2]_2[Fe(CN)_6]ClO_4$.[29,41] In K[Mn(3-MeOsalen)]$_2$[Fe(CN)$_6$]·2DMF (3-MeOsalen = *N*,*N*′-ethylenedi(3-methoxysalicylideneaminate)) of the former type, $[Fe(CN)_6]^{3-}$ makes bonds to four $[Mn(3\text{-}MeOsalen)]^+$ cations through four cyanide groups in a plane. The resulting network is a 2-D sheet based on cyclic Mn_4Fe_4 units (Fig. 10). Each potassium ion is captured by two {Mn(3-MeOsalen)(*N*)$_2$} moieties, through the methoxy oxygen atom and the phenolic oxygen atom of the 3-MeOsalen ligand, and exists in the Mn_4Fe_4 cavity. This compound showed a metamagnetic ordering (T_c = 9.2 K) due to a ferromagnetic interaction within the 2-D sheet and an antiferromagnetic interaction between the 2-D sheets. The analogous K[Mn(3-MeOsalen)]$_2$[Mn(CN)$_6$] is also a metamagnet with T_c = 16 K.

$[\{Mn(saltmen)\}_2]_2[Fe(CN)_6]ClO_4$ (saltmen = *N*,*N*′-(1,1,2,2-tetramethylethylenedi(salicylideneaminate) anion) has a similar 2-D sheet structure having $[Mn(saltmen)]_2^{2+}$ (dimeric form of $[Mn(saltn)]^+$ associated by out-of-plane Mn–O–Mn′ linkage) instead of $[Mn(3\text{-}MeOsalen)]^+$ in K[Mn(3-MeOsalen)]$_2$[Fe(CN)$_6$].[29] A ferromagnetic interaction operates in the dimeric {Mn(saltmen)}$_2$ unit and a ferromagnetic interaction operates between the adjacent Mn^{III} and Fe^{III} ions. The interaction between the 2-D sheets is also weakly ferromagnetic, resulting in a ferromagnetic ordering over the lattice (T_c = 4.5 K).

$NEt_4[Mn(5\text{-}Cl\text{-}salen)]_2[Fe(CN)_6]$ is isostructural with $K[Mn(3\text{-}MeOsalen)]_2[Fe(CN)_6]\cdot 2DMF$ and has a 2-D sheet structure based on cyclic Mn_4Fe_4 units.[42] It is a metamagnet (T_c = 10.3 K) with a ferromagnetic interaction within the 2-D sheet and an antiferromagnetic interaction between the 2-D sheets.

When 1,4,7,10,13,16-hexaoxacyclooctadecane (18-crown-6) was added to the reaction of $[Mn(acacen)(H_2O)]^+$ with $[Fe(CN)_6]^{3-}$ in 2-propanol, $[K(18\text{-crown-}6)(2\text{-}PrOH)_2][Mn(acacen)]_2[Fe(CN)_6]$ was derived.[43] The anionic $[Mn(acacen)]_2[Fe(CN)_6]^-$ part forms a 2-D sheet consisting of Mn_4Fe_4 unit similar to that in Fig. 10. The cationic $[K(18\text{-crown-}6)(2\text{-}PrOH)_2]^+$ part forms another 2-D sheet, and the cationic and anionic sheets are connected by K–PrOH···NC–Fe hydrogen bonds. This compound shows a metamagnetic ordering based on a ferromagnetic interaction within the 2-D layer and an antiferromagnetic interaction between the 2-D layers.

Thus, all the 2-D cyanide-bridged bimetallic compounds so far studied exhibit a magnetic ordering over the lattice, although their phase transition temperatures remain low because of weak magnetic interaction between 2-D sheets. The separation between 2-D sheets is important in determining the bulk magnetism; metamagnetism occurs when the intersheet separation is small (< ca. 10Å) and ferromagnetism occurs when the intersheet separation is large (> 10 Å).

3. Modulation of Magnetism by 1-D / 2-D Network Conversion

Modulation of magnetic nature by a change in network structure must be of importance for developing new molecular-based magnetic materials. Very limited systems exhibiting such magnetic modulation are described.

(1) [K(18-crown-6)(MeOH)$_2$][Mn(5-Cl-salen)(H$_2$O)(MeOH)]$_2$[Fe(CN)$_6$]·MeOH. This is a double-layer compound consisting of a cationic layer of $[K(18\text{-crown-}6)(MeOH)_2]^+$ and an anionic layer of $[Mn(5\text{-}Cl\text{-}salen)(H_2O)(MeOH)]_2[Fe(CN)_6]^-$. The anionic layer has a pseudo 2-D network extended by the Mn–OH_2···NC–Fe and Mn–MeOH···NC–Fe hydrogen-bonds.[44] In this network the metal centers are magnetically isolated from each other because of the intervenient hydrogen bonding. The methanol cap of $[Mn(5\text{-}Cl\text{-}salen)(H_2O)(MeOH)]^+$ is readily released in open air affording [K(18-crown-6)][Mn(5-Cl-salen)(H$_2$O)]$_2$[Fe(CN)$_6$]. In this compound the anionic $[Mn(5\text{-}Cl\text{-}salen)(H_2O)]_2[Fe(CN)_6]^-$ part forms another hydrogen-bonded 2-D network based on the magnetically condensed, trinuclear $Mn^{III}Fe^{III}Mn^{III}$. The water cap in the trinuclear unit is released on heating at 150 °C, affording [K(18-crown-6)][Mn(5-Cl-salen)]$_2$[Fe(CN)$_6$]. This has a 2-D network based on the cyclic Mn_4Fe_4 unit (cf. Fig. 10) and shows a magnetic ordering over the lattice (T_c = 4.0 K). The conversion of magnetically dilute $[K(18\text{-crown-}6)(MeOH)_2][Mn(5\text{-}Cl\text{-}salen)(H_2O)(MeOH)]_2[Fe(CN)_6]\cdot 4MeOH$ into magnetically condensed [K(18-crown-6)][Mn(5-Cl-salen)(H$_2$O)]$_2$[Fe(CN)$_6$] by desolvation and then into magnetically ordered [K(18-crown-6)][Mn(5-Cl-salen)]$_2$[Fe(CN)$_6$] by dehydration is schematically shown in Fig. 11.

Similarly, magnetically-condensed, trinuclear $NEt_4[Mn(5\text{-}Cl\text{-}salen)(H_2O)]_2[Fe(CN)_6]\cdot H_2O$ was converted by dehydration into $NEt_4[Mn(5\text{-}Cl\text{-}salen)]_2[Fe(CN)_6]$ that shows a metamagnetic ordering (T_c = 10.3 K).[42] The crystalline form of $NEt_4[Mn(5\text{-}Cl\text{-}salen)]_2[Fe(CN)_6]$ was prepared separately and was proved to have a 2-D sheet structure based on cyclic Mn_4Fe_4 units.

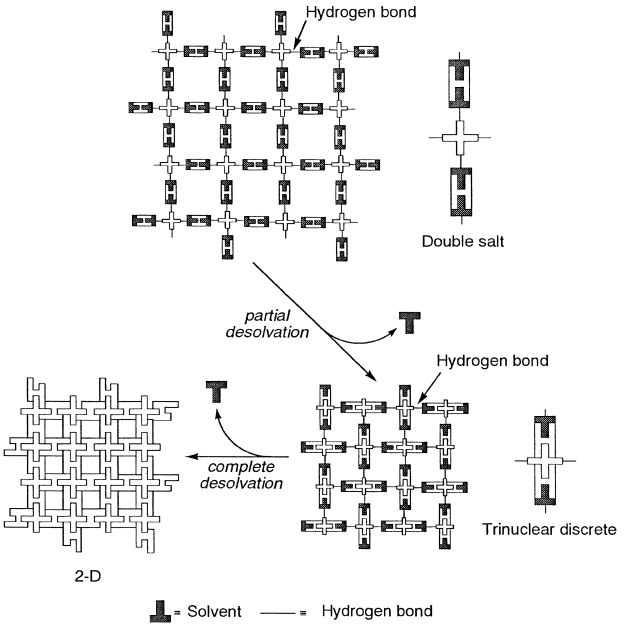

Fig. 11. Schematic view of conversion of magnetically dilute $[K(18\text{-crown-}6)(MeOH)_2][\{Mn(5\text{-Cl-salen})(H_2O)(MeOH)\}_2\{Fe(CN)_6\}].4MeOH$ to a magnetically condensed system by desolvation and then to a magnetically ordered system by dehydration.

The reverse conversion of the 2-D network compounds into the magnetically condensed and magnetically dilute compounds by hydration (and solvation), however, could not be achieved in the above two systems.

(2) $[Ni(1,1\text{-dmen})_2][Ni(1,1\text{-dmen})_2(H_2O)][Fe(CN)_6](BPDS)_{0.5}\cdot 3H_2O$ ($BPDS^{2-}$ = 4,4′-Biphenyldisulfonate). In this compound, each $[Fe(CN)_6]^{3-}$ bonds to two $[Ni(1,1\text{-dmen})_2]^{2+}$ and one $[Ni(1,1\text{-dmen})_2(H_2O)]^{2+}$ cations through three cyanide groups in the mer mode.[44] The bonding to two $[Ni(1,1\text{-dmen})_2]^{2+}$ cations forms a 1-D zigzag chain extended by the Fe–CN–Ni–NC–Fe linkage, whereas the bonding to the $[Ni(1,1\text{-dmen})_2(H_2O)]^{2+}$ cation affords $\{Ni(1,1\text{-dmen})_2(N)(H_2O)\}$ as a terminal unit attached to the 1-D chain. The aqua molecule in the terminal unit is involved in the hydrogen bond to a cyanide nitrogen (N2) of the adjacent chain, affording a pseudo 2-D network structure (Fig. 12). This network structure is related to the 2-D square-sheet structure of $[Ni(1,1\text{-dmen})_2]_2[Fe(CN)_6]X\cdot nH_2O$ (Fig. 8), by replacing two Fe–CN–Ni linkages in the square unit with hydrogen-bonding Fe–CN···H_2O–Ni linkages. The counter anion $BPDS^{2-}$ exists between two pseudo 2-D sheets in a planar arrangement, with one sulfonate group situated above one pseudo square unit and another group above the adjacent pseudo square unit. The pseudo 2-D network structure in Fig. 12 is associated with the $BPDS^{2-}$ counter anion. That is, this anion necessitates an expansion of the square unit of Fig. 8 along the anion molecule, because the S···S separation of $BPDS^{2-}$ is ca. 10.8 Å that is larger than the center-center separation of adjacent square units (10.1 – 10.4 Å). This compound shows a metamagnetic ordering (T_c = 4.7 K). The saturation magnetization curve has an inflection around 4 kG due to the phase transition from metamagnetic ordering to ferromagnetic ordering.

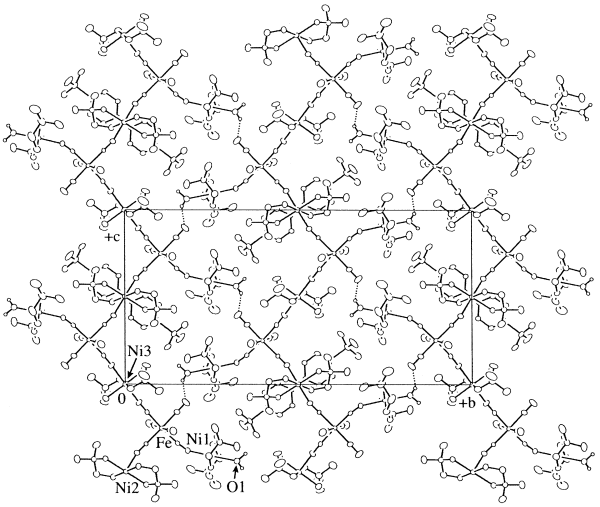

Fig. 12. Pseudo 2-D network structure of $[Ni(1,1\text{-dmen})_2]_2[Fe(CN)_6](BPDS)_{0.5}\cdot 4H_2O$.

$[Ni(1,1\text{-dmen})_2][Ni(1,1\text{-dmen})_2(H_2O)][Fe(CN)_6](BPDS)_{0.5}\cdot 3H_2O$ shows three ν(CN) bands at 2170, 2138 and 2122 cm^{-1} in accord with a low symmetry about the Fe ion. It was dehydrated at 150 °C to anhydrous $[Ni(1,1\text{-dmen})_2]_2[Fe(CN)_6](BPDS)_{0.5}$. The anhydrate shows two ν(CN) bands at 2139 and 2112 cm^{-1}, suggesting that the dehydration accompanies the conversion of the pseudo 2-D sheet structure of Fig. 12 into a 2-D grid structure in Fig. 8. The anhydrate adsorbed atmospheric moisture in open air to afford the dihydrate $[Ni(1,1\text{-dmen})_2]_2[Fe(CN)_6](BPDS)_{0.5}\cdot 2H_2O$. The dihydrate showed three ν(CN) bands at 2139, 2123 and 2112 cm^{-1} and two ν(O-H) bands at 3544 and 3469 cm^{-1}, indicating that it has essentially the same pseudo 2-D network as that in Fig. 12. The anhydrate and the dihydtate can be interconverted by hydration and dehydration treatment.

The $\chi_M T$ vs T curve of the anhydrate showed a rapid increase below 10 K to a large maximum value of 405.5 cm^3 K mol^{-1} (57.0 μ_B) at 8.7 K. The field-dependence of magnetization at 2 K indicated an inflection at ca. 200 G and then a sharp increase with the applied field (Fig. 13, a). The magnetic nature of the anhydrate resembles that of ferromagnetic $[Ni(1,1\text{-dmen})_2]_2[Fe(CN)_6]X\cdot nH_2O$ of the 2-D square sheet structure.[38] The inflection near 200 G means the occurrence of a weak antiferromagnetic interaction between the 2-D sheets. The dihydrate shows metamagnetic nature. Its saturation magnetization curve has an inflection at 3 kG due to the spin flip from a metamagnetic ordering to a ferromagnetic ordering (Fig. 13, b).

Thus, the reversible ferromagnetism/metamagnetism interconversion is first established in the present magnetic system. The 2-D grid structure of the anhydrate is unstable, because of unbalance in the electrostatic interaction between the positive charge of the square unit and the negative charge of the sulfonate group of $BPDS^{2-}$, and reverts to the hydrogen-bonded pseudo 2-D structure by adsorbing atmospheric moisture.

4. Three-Dimensional Network Compounds

(1) $[Ni(L)_2]_3[Fe^{II}(CN)_6]X_2$ (L = en, tn; X = ClO_4^-, PF_6^-). These complexes were obtained as purple crystals by the reac-

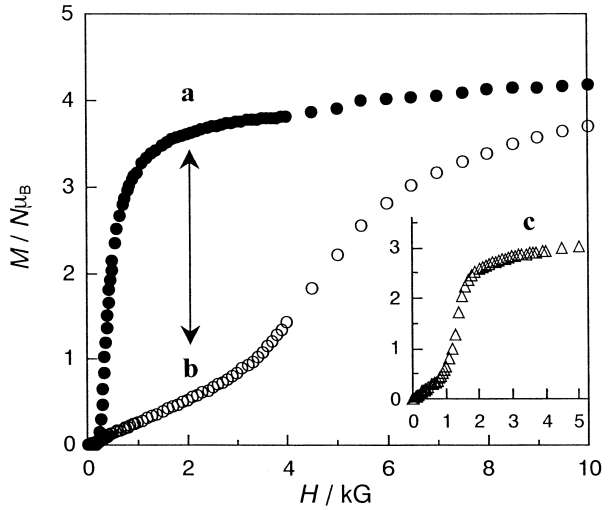

Fig. 13. M vs H curves of (a) anhydrous $[Ni(1,1\text{-dmen})_2]_2[Fe(CN)_6](BPDS)_{0.5}$ and (b) its dihydrate at 2 K. The insert (c) is the M vs H curve for $[Ni(1,1\text{-dmen})_2]_2[Fe(CN)_6](BPDS)_{0.5}\cdot 4H_2O$.

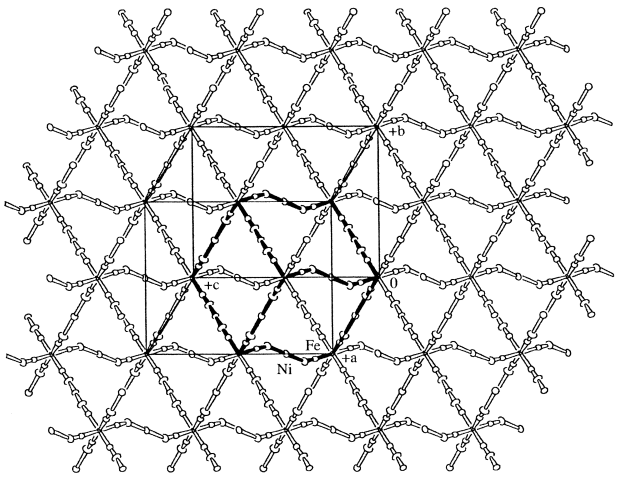

Fig. 14. 3-D cubic network of $[Ni(en)_2]_3[Fe(CN)_6](ClO_4)_2$.

tion of $[Ni(L)_3]X_2$ (L = en or tn; X = ClO_4^- or PF_6^-) and $K_4[Fe^{II}(CN)_6]$ in an aqueous solution.[45] In the crystal of $[Ni(en)_2]_3[Fe^{II}(CN)_6](PF_6)_2$, each $[Fe(CN)_6]^{4-}$ makes bonds to six $[Ni(en)_2]^{2+}$ cations through all the cyanide groups, forming a 3-D network structure based on a cubic Fe_8Ni_{12} unit (Fig. 14). The unit has eight Fe^{II} ions at the corners and twelve $[Ni(en)_2]^{2+}$ cations at the center of the edges. The Fe^{II}–C bond distance (1.913 Å) is short relative to the Fe^{III}–C distance of related compounds (> 1.94 Å), indicating a strong π back-donation from Fe^{II} to vacant π orbital of cyanide ion. The nearest Fe···Ni, Fe···Fe and Ni···Ni separations of the cubic unit are 4.954, 9.908 and 9.908 Å, respectively. Two PF_6^- anions are captured in the Fe_8Ni_{12} cube. All the complexes show one ν(CN) band at 2060 cm^{-1}. In accord with the high symmetry of the network structure, all the complexes show one ν(CN) band at 2060 cm^{-1}.

The $\chi_M T$ value at room temperature is 3.50 cm^3 K mol^{-1} (5.29 μ_B per $FeNi_3$) which is practically independent of temperature down to 120 K but gradually increased with further decreasing temperature up to 5.05 cm^3 K mol^{-1} (6.34 μ_B) at 2.0 K. Thus, ferromagnetic interaction operated between the adjacent Ni^{II} centers through diamagnetic Fe^{II}. Analogous 3-D cubic network compounds having paramagnetic $[M^{II}(CN)_6]^{4-}$ must be important, but such compounds have not yet been obtained.

(2) $[Ni(dipn)]_2[Ni(dipn)(H_2O)][M(CN)_6]_2\cdot 6H_2O$ (dipn = Di(1,3-propylene)triamine; M^{III} = Fe, Co). In order to construct a 3-D bimetallic network based on $[M(CN)_6]^{3-}$ as the bridging constituent, the second metal as the connecting constituent must make available at least three vacant sites for accepting cyanide nitrogen atoms from adjacent $[M(CN)_6]^{3-}$ ions. Such geometrical requirement about the connector can be effected by the use of $[Ni(triamine)]^{2+}$. The complexes were obtained as good crystals by reacting stoichiometric amounts of the constituents in an aqueous DMF solution.[46] $[Ni(dipn)]_2[Ni(dipn)(H_2O)][Fe(CN)_6]_2\cdot 6H_2O$ shows two ν(CN) bands at 2153 and 2123 cm^{-1} and $[Ni(dipn)]_2[Ni(dipn)(H_2O)][M(CN)_6]_2\cdot 6H_2O$ shows two ν(CN) bands at 2140 and 2138 cm^{-1} In both compounds, each $[M(CN)_6]^{3-}$ bonds to three $[Ni(1)(dipn)]^{2+}$ cations and one $[Ni(2)(dipn)(H_2O)]^{2+}$ cation. In both $\{Ni(1)(dipn)(N)_3\}$ and $\{Ni(2)(dipn)(H_2O)(N)_2\}$ units the dipn ligand assumes the mer coordination mode. The M–CN–Ni(1) linkages extend on the bc plane to form a 2-D sheet consisting of cyclic Ni_4M_4 and Ni_2M_2 units (Fig. 15(a)), and the 2-D sheets are connected by the M–CN–Ni(2) linkage providing a 3-D network structure (Fig. 15 (b)).

$[Ni(dipn)]_2[Ni(dipn)(H_2O)][Fe(CN)_6]_2\cdot 6H_2O$ is a ferromagnet exhibiting spontaneous magnetization below T_c = 7.8 K. It is of value to consider the reason why its magnetic phase-transition temperature remains low and even lower than those of 2-D magnetic compounds, $[Ni(1,1\text{-dmen})_2]_2[Fe(CN)_6]X\cdot nH_2O$ (T_c: 8.5 – 20.3 K). It must be pointed out that the exact symmetry about the Fe in the assembly is C_{2v} but not O_h. Under the C_{2v} symmetry, the d_π character orbitals (d_{xy}, d_{xz}, d_{yz}) split into $a_2(d_{xy})$, $b_1(d_{xz})$ and $b_2(d_{yz})$ orbitals. If the Fe^{III} has one unpaired electron on d_{xy} orbital, the Fe^{III} can interact with the Ni^{II} centers on the xy plane through cyanide bridge but not with the Ni^{II} centers on the z axis (Fig. 16). The same situation occurs when Fe^{III} has one unpaired electron on d_{xz} or d_{yx} orbital. Therefore, a 2-D magnetic ordering occurs in the compound irrespective of electronic configuration of Fe^{III}.

(3) $[Mn(dien)]_3[Cr(CN)_6]_2\cdot 2H_2O$ The above discussion suggests that $[Cr(CN)_6]^{3-}$ with the $(d_\pi)^3$ electronic configuration must be a good bridging constituent in the design of high T_c magnetic material. Analogous compounds of $[Ni(dien)]^{2+}$ and $[Cr(CN)_6]^{3-}$ are unknown, but $[Mn(dien)]_3[Cr(CN)_6]_2\cdot 2H_2O$ can be used for inspecting the significance of $[Cr(CN)_6]^{3-}$ in 3-D magnetic ordering.[46] This compound was obtained by the reaction of Mn^{II} chloride, dien and $K_3[Cr(CN)_6]$ in the 3:3:2 stoichiometry in an aqueous solution under anaerobic conditions. It has two ν(CN) bands at 2152 and 2124 cm^{-1}.

The $\chi_M T$ value (per Mn_3Cr_2) decreased with decreasing temperature to a minimum value of 14.34 cm^3 K mol^{-1} (10.7 μ_B) at 170 K, increased to a large maximum of 3384 cm^3 K mol^{-1} (164.5 μ_B) at 46 K and then decreased below this temperature. The decrease in the $\chi_M T$ value below 46 K is the result of a saturation of magnetic susceptibility. The minimum $\chi_M T$ value is compared to the spin-only value of 12.38 cm^3 K mol^{-1} (9.95

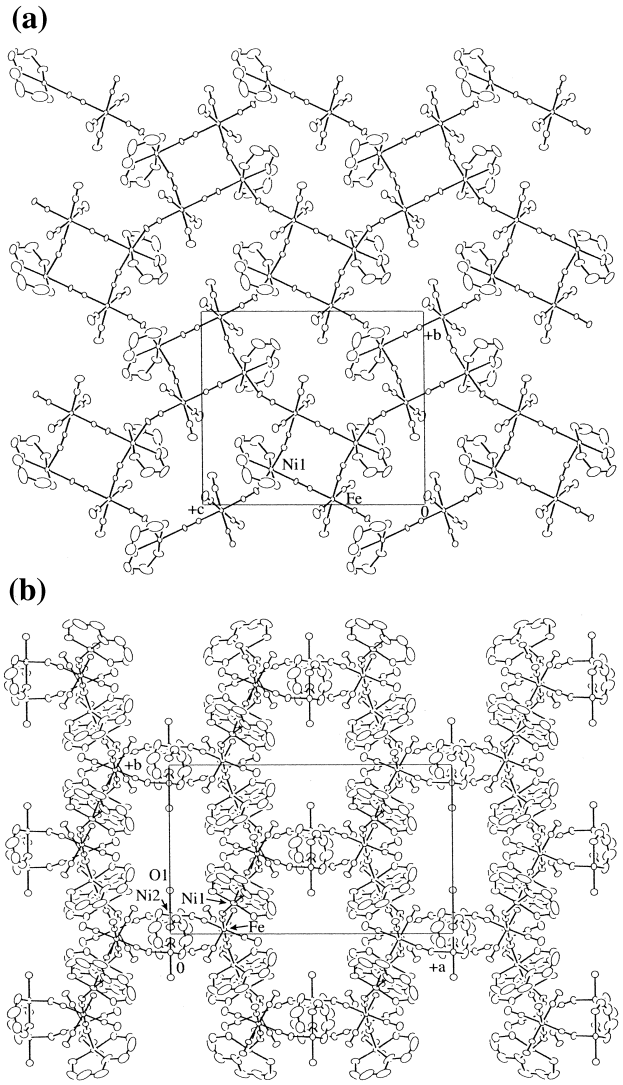

Fig. 15. The network structure of $[\{Ni(dipn)\}_2\{Ni(dipn)(H_2O)\}][Fe(CN)_6]_2\cdot 6H_2O$; (a) a projection on *bc* plane and (b) a projection on *ab* plane.

μ_B) for $S_T = 9/2$ arising from antiferromagnetic coupling between the adjacent Mn^{II} and Cr^{III} ions. The antiferromagnetic interaction is explained by the $d_\pi(Mn) \parallel d_\pi(CN) \parallel d_\pi(Cr)$ superexchange pathway. The abrupt increase in $\chi_M T$ below 70 K is the indication of a magnetic ordering over the lattice. Magnetization studies indicated that this is a ferrimagnet with T_c = 63 K that is very high when compared with the T_c = 7.8 K of $[Ni(dipn)]_2[Ni(dipn)(H_2O)][Fe(CN)_6]_2\cdot 6H_2O$. Despite lack of structural information for the former and the difference in the cationic constituent between the two, the above work suggests $[Cr(CN)_6]^{3-}$ to be a more efficient constituent than $[Fe(CN)_6]^{3-}$ in providing high T_c magnetic material.

(4) $[Mn(L)]_3[Cr(CN)_6]_2\cdot nH_2O$ (L = en, glya (Glycine Amide)). In $[\{Ni(dipn)\}_2\{Ni(dipn)(H_2O)\}][M(CN)_6]_2\cdot 6H_2O$ (M = Fe, Co) discussed above, the $\{Ni(dipn)(N)_3\}$ entity assumes the mer configuration to allow a two-dimensional extension about the Ni ion.[46] If the connecting constituent has one bidentate capping ligand like $[M(en)]^{2+}$, it provides four vacant sites for accepting cyanide groups along *x*, *y* and *z* axes

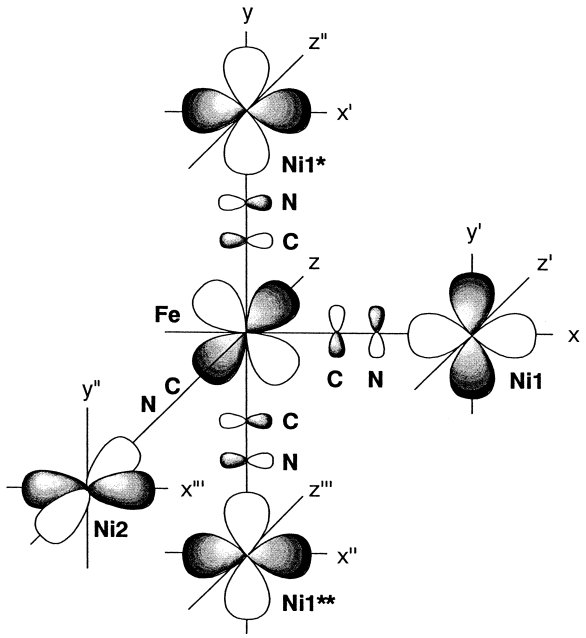

Fig. 16. A schematic presentation of 2-D magnetic interaction in $[\{Ni(dipn)\}_2\{Ni(dipn)(H_2O)\}][Fe(CN)_6]_2\cdot 6H_2O$.

and allows a three-dimensional extension about the metal center. Such a 3-D extension about the connecting metal center must be important for providing high T_c magnetic material.

$[Mn(L)]_3[Cr(CN)_6]_2\cdot nH_2O$ (L = en, glya)[47,48] were prepared as good crystals by the reaction of Mn^{II} chloride, the supporting ligand (en or glya) and $K_3[Cr(CN)_6]$ in the 3:3:2 molar ratio in aqueous solution under argon. The IR spectra of the two compounds have one ν(CN) band near 2150 cm^{-1}, suggesting that all the cyanide groups of $[Cr(CN)_6]^{3-}$ are involved in bridging. It is generally considered that amine nitrogen has a low affinity toward high-spin Mn^{II}, but the coordination of en and glya to Mn^{II} through amine nitrogen is evidenced by X-ray crystallography.

Two crystallographically-independent $[Mn(en)]^{2+}$ units, $[Mn(1)(en)]^{2+}$ and $[Mn(2)(en)]^{2+}$, exist in the crystal of $[Mn(en)]_3[Cr(CN)_6]_2\cdot 4H_2O$. The asymmetric unit consists of one $[Cr(CN)_6]^{3-}$ ion, one $[Mn(1)(en)]^{2+}$, one half of $[Mn(2)(en)]^{2+}$ and two water molecules (Fig. 17(a)). $[Cr(CN)_6]^{3-}$ makes bonds to six Mn^{II} centers with all the cyanide groups. The geometry about each Mn is pseudo octahedral $\{Mn(en)(N)_4\}$ with a chelating en ligand and four cyanide nitrogen atoms from adjacent $[Cr(CN)_6]^{3-}$ ions. In the lattice, a 3-D network structure is formed which is based on a defective cubane unit with three Cr atoms, three Mn(1) atoms and one Mn(2) atom at the seven corners; one corner of the cubane unit is lacking (Fig. 17(b)). The lattice water molecules reside in the cavity.

The magnetic behavior of $[Mn(en)]_3[Cr(CN)_6]_2\cdot 4H_2O$ is shown in Fig. 18 (left) in $\chi_M T$ vs *T* and χ_M vs *T* plots. The $\chi_M T$ value decreased with decreasing temperature to a minimum value of 12.04 cm^3 K mol^{-1} (9.82 μ_B) at 156 K, increased to a large maximum value of 5671 cm^3 K mol^{-1} (213 μ_B) at 50 K and then decreased below this temperature. The minimum $\chi_M T$ value agrees well with the spin-only value of 12.38 cm^3 K mol^{-1} (9.95 μ_B) for antiferromagnetically coupled Mn_3Cr_2 (S_T

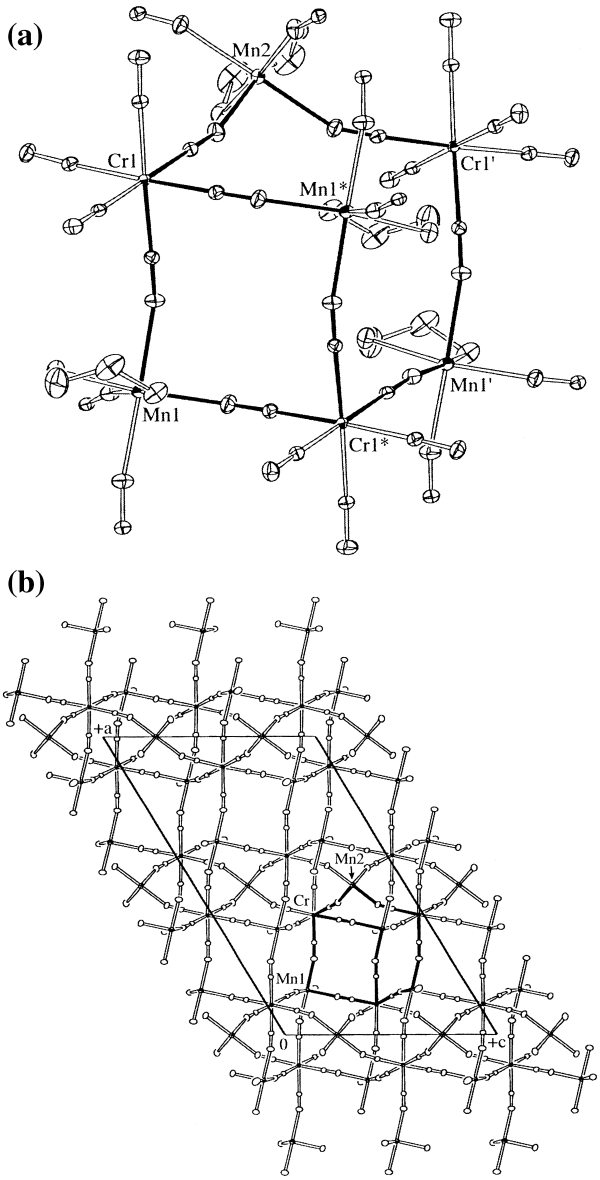

Fig. 17. Projection of (a) Mn_4Cr_3 defective cubane unit and (b) 3-D network structure of $[Mn(en)]_3[Cr(CN)_6]_2 \cdot 4H_2O$.

= 9/2). Evidently, an antiferromagnetic interaction operates between the adjacent Mn^{II} and Cr^{III} centers through the $d_\pi(Mn) \parallel d_\pi(CN) \parallel d_\pi(Cr)$ pathway. The abrupt increase in $\chi_M T$ around 70 K means the onset of a long-range magnetic ordering, and magnetization studies (FM, RM and ZFCM) have confirmed that this is a ferrimagnet with T_c = 69 K (Fig. 18, right). The decrease in $\chi_M T$ below 50 K arises from the saturation of magnetic susceptibility.

$[Mn(glya)]_3[Cr(CN)_6]_2 \cdot 2.5H_2O$ has a similar 3-D network structure based on a defect cubane unit.[48] This also shows a ferrimagnetic ordering over the lattice with T_c = 71 K. To the best of our knowledge, this is the highest T_c among the structurally characterized molecular magnets.

A close structural analogy of $[Mn(L)]_3[Cr(CN)_6]_2 \cdot nH_2O$ (L = en, glya) to Prussian blue compounds of the type of $A^{II}{}_3[B^{III}(CN)_6]_2 \cdot nH_2O$ has been pointed out. This is obvious when the Prussian blue compounds are formulated as $[A(H_2O)_2]_3[B(CN)_6]_2 \cdot (n\text{-}6)H_2O$. We have confirmed that $Mn_3[Fe(CN)_6]_2 \cdot 12H_2O$ (= $[Mn(H_2O)_2]_3[Cr(CN)_6]_2 \cdot 6H_2O$) exhibits a ferrimagnet ordering at T_c = 63 K.

Conclusion

From above studies on cyanide-bridged bimetallic compounds of various networks, some important factors relating to magnetic ordering in the bulk and magnetic nature can be drawn. 1-D network compounds generally show no magnetic ordering. 2-D network structures lead to a magnetic ordering over the lattice, ferromagnetism or metamagnetism depending upon the intersheet separation, but the magnetic phase transition temperature T_c remains low owing to weak intersheet magnetic interaction. 3-D network has a bright prospect of developing high T_c magnetic compounds. The local geometry and electronic configuration of the bridging and the connecting metal center must also be taken into consideration for providing high T_c compounds, as shown by $[Ni(dipn)]_2[Ni(dipn)(H_2O)][Fe(CN)_6]_2 \cdot 6H_2O$ and $[Mn(dien)]_3[Cr(CN)_6]_2 \cdot 2H_2O$.[46]

Along with the production of high T_c magnetic compounds, an important subject in the study of "the second generation" of molecular-based magnets is to produce unique magnetic systems that cannot be realized with magnetic materials common-

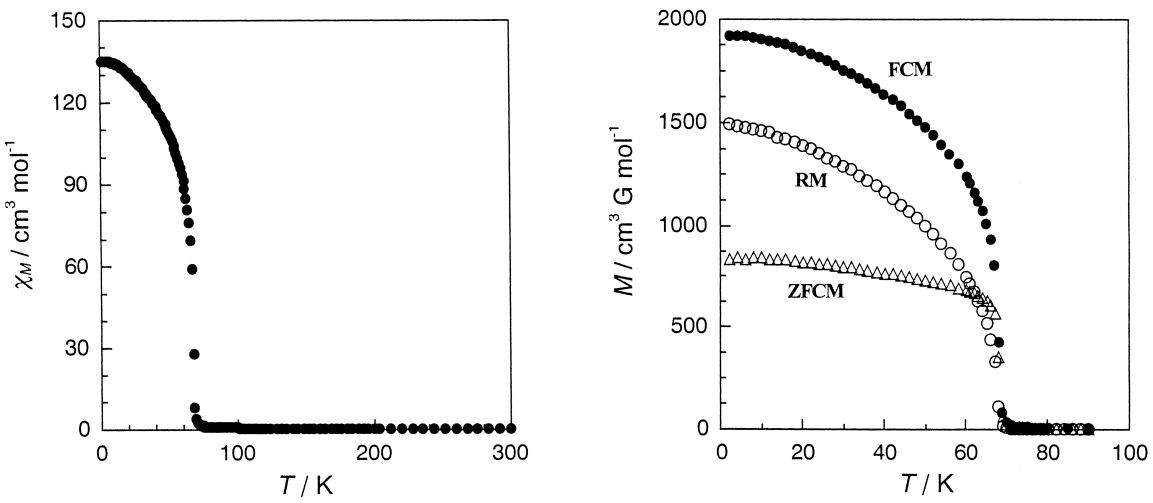

Fig. 18. χ_M vs T curve (left) and FM, RM and ZFCM (right) for $[Mn(en)]_3[Cr(CN)_6]_2 \cdot 4H_2O$.

ly used (metals and metal oxides). One characteristic of complex-based magnets is optical absorption by the constituting metal center. Sato et al. first reported a photo-induced modulation of magnetic nature of $K_{0.2}Co_{1.4}[Fe(CN)_6]\cdot 6.9H_2O$;[49] a conversion of the diamagnetic $Fe^{II}(S = 0)$–CN–$Co^{III}(S = 0)$ site into paramagnetic $Fe^{III}(S = 1/2)$–CN–$Co^{II}(S = 3/2)$ by irradiation of red light and a partial reverse conversion by irradiation of blue light. Our cyanide-bridged bimetallic magnetic compounds have been obtained as colored transparent single crystals (transparent magnets), which allow us to study Faraday effect and magnetic-dipolar transitions of metal ion in magnetically ordered systems. Thus, "optospinics" (optical spin-manipulated electronics) is one promising prospect in the study of "the second generation" of molecular-based magnets.[50] Another characteristic of molecular magnets is the "soft" nature of the network structure that may be changeable by any external cause to exhibit variable magnetism, as illustrated by $[Ni(1,1\text{-dmen})_2]_2[Fe(CN)_6](BPDS)_{0.5}\cdot 4H_2O$.[44] Recently we have noticed that 3-D trimetallic compounds of a 3d–3d′–4f system show very rare magnetic properties.[51] Basic studies on such new systems are also important for developing advanced magnetic materials.

The authors thank Dr. N. Fukita, Mr. N. Usuki and Mr. M. Yamada (Kyushu Univ.), Dr. H. Miyasaka (Tokyo Metropolitan Univ.), Prof. T. Ito (Tohoku Univ.) and Prof. T. Enoki (Tokyo Institute of Technology) for collaboration. This work was supported by a Grant-in-Aid for Scientific Research on Priority Area "Metal-assembled Complexes (No. 10149106)," a Grant-in-Aid for COE Research "Design and Control of Advanced Molecular Assembly System (No. 08CE2005)" and a Grant-in-Aid for Scientific Research Program (No. 13640561) from the Ministry of Education, Culture, Sports, Science and Technology. One of the authors (M. Ohba) thanks Precursory Research for Embryonic Science and Technology (PRESTO), JST for financial support.

References

1 J. S. Miller, A. J. Epstein, and W. M. Reiff, *Chem. Rev.*, **88**, 201 (1988).

2 O. Kahn, Y. Pei, M. Verdaguer, J. P. Renard, and J. Sletten, *J. Am. Chem. Soc.*, **110**, 782 (1988).

3 A. Caneschi, D. Gatteschi, J. P. Renard, P. Rey, and R. Sessoli, *Inorg. Chem.*, **28**, 1976 (1989); A. Caneschi, D. Gatteschi, J. P. Renard, P. Rey, and R. Sessoli, *ibid.*, **28**, 2940 (1989); A. Caneschi, D. Gatteschi, J. P. Renard, P. Rey, and R. Sessoli, *ibid.*, **28**, 3313 (1989).

4 "Magnetic Molecular Materials," NATO ASI Series 198, ed by D. Gatteschi, O. Kahn, J. S. Miller, and F. Palacios, Kluwer Academic Pub., Dordrecht (1990).

5 "Molecular Magnetism," ed by O. Kahn, VCH, New York (1993).

6 "Molecule-based Magnetic Materials," ACS Symposium Series 644, ed by M. M. Turnbull, T. Sugimoto, and L. K. Thompson, Am. Chem. Soc., Washington (1996).

7 "Molecular Magnetism: New Magnetic Material," ed by K. Itoh and M. Kinoshita, Gordon & Breach Sci. Pub., Amsterdam (2000).

8 O. Kahn, Y. Pei, and Y. Journaux, in "Inorganic Materials," ed by D. W. Bruce and D. O'Hare, John Wiley & Sons, (1992), p. 60.

9 K. R. Dumbar and R. A. Heinetz, *Prog. Inorg. Chem.*, **45**, 283 (1997).

10 D. Davidson and L. A. Welo, *J. Phys. Chem.*, **32**, 1191 (1928).

11 R. Klenze, B. Kanellalopulos, G. Trageser, and H. H. Eysel, *J. Chem. Phys.*, **72**, 5819 (1980).

12 V. Gadet, T. Mallah, I. Castro, and M. Verdaguer, *J. Am. Chem. Soc.*, **114**, 9213 1992.

13 V. Gadet, M. Bujoli-Deeuff, L. Force, M. Verdaguer, K. E. Malkhi, A. Deroy, J. O. Besse, C. Chappert, P. Veillet, J. P. Renard, and P. Beauvillain, in "Molecular Magnetic Material," NATO ASI Series 198, ed by D. Gatteschi, O. Kahn, J. S. Miller and F. Palacios, Kluwer Academic Pub., Dordrecht (1991), p. 281.

14 W. D. Griebler and D. Babel, *Z. Naturforsch. B: Chem. Sci.*, **87**, 832 (1982).

15 W. R. Entley and G. S. Girolani, *Inorg. Chem.*, **33**, 5165 (1994).

16 W. R. Entley and G. S. Girolani, *Science*, **268**, 397 (1995).

17 T. Mallah, S. Thiebaut, M. Verdaguer, and P. Veillet, *Science*, **262**, 1554 (1993).

18 S. Entley, T. Mallah, R. Ouahes, P. Veillet, and M. Verdaguer, *Nature*, **378**, 701 (1995).

19 O. Kahn, *Nature*, **378**, 667 (1995).

20 O. Sato, T. Iyoda, A. Fujishima, and K. Hashimoto, *Science*, **271**, 49 (1996); *ibid.*, **271**, 704 (1996).

21 M. Ohba, N. Maruono, H. Ōkawa, T. Enoki, and J. M. Latour, *J. Am. Chem. Soc.*, **116**, 11566 (1994).

22 M. Ohba, N. Fukita and H. Ōkawa, *J. Chem. Soc., Dalton Trans.*, **1997**, 1733.

23 B. N. Figgis, E. D. Kucharski and M. Virtis, *J. Am. Chem. Soc.*, **115**, 176 (1993).

24 C. A. Daul, P. Day, B. N. Figgis, H. U. Gudel, F. Herren, A. Ludi, and P. A. Reynords, *Proc. R. Soc. London, Ser. A*, **419**, 205 (1998).

25 K. V. Langenberg, S. R. Batten, K. J. Berry, D. C. R. Hockless, B. Moubaraki and K. S. Murray, *Inorg. Chem.*, **36**, 5006 (1997).

26 M. Ohba, N. Usuki, N. Fukita, and H. Ōkawa, *Inorg. Chem.*, **37**, 3349 (1998).

27 H. Ōkawa and M. Ohba, in "Molecule-Based Magnetic Materials," ACS Symposium Series 644, ed by M. M. Turnbull, T. Sugimoto, and L. K. Thompson, Am. Chem. Soc., Washington (1996), p.319.

28 M. Re, E. Gallo, C. Floriani, H. Miyasaka and N. Matsumoto, *Inorg. Chem.*, **35**, 6004 (1996).

29 H. Miyasaka, N. Matsumoto, H. Ōkawa, N. Re, E. Gallo, and C. Floriani, *J. Am. Chem. Soc.*, **118**, 981 (1996).

30 E. Colacio, J. M. Dominguez-Vera, M. Ghazi, R. Kivekas, and J. M. Moreno, *Chem. Commun.*, **1998**, 1071.

31 H. Kou, D. Liao, P. Cheng, Z. Jiang, S. Yan, G. Wang, X. Yao and H. Wang, *J. Chem. Soc., Dalton Trans.*, **1997**, 1503.

32 M. Ohba and H. Ōkawa, *Coord. Chem. Rev.*, **198**, 313 (2000).

33 S. Ferlay, T. Mallah, J. Vaissermann, F. Bartolome, P. Veillet, and M. Verdaguer, *Chem. Commun.*, **1996**, 2482.

34 N. Fukita, M. Ohba, and H. kawa, *Mol. Cryst. Liq. Cryst.*, **342**, 217 (2000).

35 S. E. Fallah, E. Rentschler, A. Caneschi, R. Sessoli, and D.

Gatteschi, *Angew. Chem., Int. Ed. Engl.*, **35**, 1947 (1996).
36 M. Ohba, H. Ōkawa, T. Ito and A. Ohto, *J. Chem. Soc., Chem. Commun.*, **1995**, 1545.
37 M. Ohba and H. Ōkawa, *Mol. Cryst. Liq. Cryst.*, **286**, 101 (1996).
38 M. Ohba, N. Fukita, H. Ōkawa, and Y. Hashimoto, *J. Am. Chem. Soc.*, **119**, 1011 (1997).
39 N. Usuki, M. Ohba, and H. Ōkawa, unreported data.
40 H. Z. Kou, W. Bu, D. Liao, Z. Jiang S. Yan Y. Fan, and H. Wang, *J. Chem. Soc., Dalton trans.*, **1998**, 4161.
41 H. Miyasaka, N. Matsumoto, H. Ōkawa, N. Re, E. Gallo, and C. Floriani, *Angew. Chem., Int. Ed. Engl.*, **34**, 1446 (1995).
42 H. Miyasaka, N. Matsumoto, N. Re, E. Gallo and C. Floriani, *Inorg. Chem.*, **36**, 670 (1997).
43 H. Miyasaka, H. Ōkawa, A. Miyazaki and T. Enoki, *Inorg. Chem.*, **37**, 4878 (1998).
44 N. Usuki, M. Ohba and H. Ōkawa, submitted for publication.
45 N. Fukita, M. Ohba, H. Ōkawa, K. Matsuda and H. Iwamura, *Inorg. Chem.*, **37**, 842 (1998).
46 M. Ohba, M. Yamada, and H. Ōkawa, submitted to publication.
47 M. Ohba, N. Usuki, N. Fukita, and H. Ōkawa, *Angew. Chem., Int. Ed.*, **38**, 1795 (1999).
48 N. Usuki, M. Yamada, M. Ohba, and H. Ōkawa, *J. Solid State Chem.*, **159**, 328 (2001).
49 O. Sato, T. Iyoda, A. Fujishima, and K. Hashimoto, *Science*, **272**, 704 (1996).
50 M. Verdaguer, *Science*, **272**, 698 (1996).
51 M. Ohba et. al, unreported data.

Hisashi Ōkawa was born in 1941 in Miyazaki, Japan. He gained his B. Sc. in 1964, M. Sc. in 1965 and his D. Sc. in 1969 from Kyushu University. He was appointed Lecturer in the Faculty of Science at Kyushu University in 1970, promoted to Associate Professor in 1972 and is currently Professor of Coordination Chemistry Laboratory. In 1998 he was a Visiting Professor at the Institute for Molecular Science in Okazaki. His research interests lie in the area of coordination chemistry, bioinorganic chemistry and magnetochemistry. In 1996 Ōkawa was awarded a Daiwa Award by the Daiwa Anglo-Japanese Foundation, together with Professor David E. Fenton of the University of Sheffield, for researches on bimetallic biosite modelling. He was also awarded Chemical Society of Japan Award in 2000 for his works on multinuclear metal complexes.

Masaaki Ohba was born in 1969 at Amagi in Fukuoka, Japan. He received his B. Sc. in 1991, M. Sc. in 1993 and D. Sc. in 1996 from Kyushu University. He was also received Research Fellowships for Young Scientists during 1994–1996 from Japan Society for the Promotion of Science (JSPS). He has been appointed Research Associate at Kyushu University since 1996. Now he is also working at Precursory Research for Embryonic Science and Technology (PRESTO), Japan Science and Technology Corporation (JST). His research interest lies in coordination chemistry and his current focus is placed on solid state physical properties, especially magnetic and magneto-optical aspects of metal-assembled compounds.